Published in final edited form as:
J Neurosci Methods. 2014 January 30; 222: 82–90. doi:10.1016/j.jneumeth.2013.10.014.

Neural Circuits with Long-Distance Axon Tracts for Determining Functional Connectivity

Min D. Tang-Schomer[a], **Paul Davies**[b], **Daniel Graziano**[a], **Amy E. Thurber**[c], and **David L. Kaplan**[a,*]

[a]Tufts University, Department of Biomedical Engineering, Medford, MA 02155

[b]Tufts University, Neuroscience Center, Boston

[c]Tufts University, Sackler School of Graduate Biomedical Sciences, Program in Cell, Molecular, and Developmental Biology, Boston, MA 02111

Abstract

The cortical circuitry in the brain consists of structurally and functionally distinct neuronal assemblies with reciprocal axon connections. To generate cell culture-based systems that emulate axon tract systems of an *in vivo* neural network, we developed a living neural circuit consisting of compartmentalized neuronal populations connected by arrays of two millimeter-long axon tracts that are integrated on a planar multi-electrode array (MEA). The millimeter-scale node-to-node separation allows for pharmacological and electrophysiological manipulations to simultaneously target multiple neuronal populations. The results show controlled selectivity of dye absorption by neurons in different compartments. MEA-transmitted electrical stimulation of targeted neurons shows ∼46% increase of intracellular calcium levels with 20 Hz stimulation, but ∼22% decrease with 2k Hz stimulation. The unique feature of long distance axons promotes *in vivo*-like fasciculation. These axon tracts are determined to be inhibitory afferents by showing increased action potential firing of downstream node upon selective application of γ-aminobutyric acid (GABA) to the upstream node. Together, this model demonstrates integrated capabilities for assessing multiple endpoints including axon tract tracing, calcium influx, network architecture and activities. This system can be used as a multi-functional platform for studying axon tract-associated CNS disorders *in vitro*, such as diffuse axonal injury after brain trauma.

Keywords

Micropattern; Axon tract; Inhibitory afferent; Electrical stimulation; Calcium imaging; Interface

1.Introduction

Neural circuits in the body are formed by discrete populations of neural cell assemblies connected with stereotypically organized axon tracts. Compartmentalization of neural assemblies, the nucleus in the central nervous system (CNS) and ganglia in the peripheral nervous system, forms the basis for functional modules, while the white matter axon tracts and nerves transmit electrical signals between these functional units. Damages to a discrete axon tract have a profound, yet poorly understood, effect on the network behavior of its circuitry, as manifested in post-traumatic stress disorder (PTSD) after traumatic brain injury (TBI) (Rauch et al., 2006). Indeed, diffuse axonal injury, identified as damage or dysfunction of axons throughout the white matter, is the most common and important

*corresponding author: david.kaplan@tufts.edu.

pathology in TBI (Strich., 1956, Adams et al., 1989, Christman et al., 1994, Gentleman et al., 1995). Conversely, neural plasticity, a neural network's adaptive capability of remodeling and reorganization, provides a potential mechanism as a basis for rehabilitation therapy to restore lost function (Takatsuru et al., 2009, Ghosh et al., 2009). Pioneering work involving the relationship of a specific axon pathway to overall network behavior were performed in simple circuits such as reciprocally inhibitory interneurons that produces oscillatory movements in lower organisms (Friesen., 1994). The brain circuitry's complexity has made it difficult to relate dysfunction of a discrete pathway to system-level changes of neural networks. Thus, it is desirable to generate cell culture-based systems that emulate the basic organization of *in vivo* circuitry, with physically separated neuronal populations and controlled axon tracts. Further, it is necessary to access and manipulate individual network components in order to perform mechanistic studies.

Micro-patterned surfaces have been used in neuronal cultures to fabricate neural networks with pre-determined geometry. The patterns provide selective surfaces to control neuronal attachment and growth (Jung et al., 2001, Li et al., 2003,Corey and Feldman., 2003). Surface patterning methods include microfluidic channels (Taylor et al., 2005), laser-ablated microgrooves (Corey et al., 1991), silane coupling-mediated covalent binding (Kleinfeld et al., 1988,Ravenscroft., 1998) or microcontact printing of cell adhesion molecules such as polylycine (Jun et al., 2007) and laminin (Hammarback et al., 1985). However, long-term confinement of neuronal cultures to pre-determined geometry on a planar surface remains challenging due to detachment or degradation of surface adhesion molecules, surface masking by serum or cell secreted proteins, as well as cell migration and formation of axon bundles between cell clusters that distort the original pattern design (Ravenscroft., 1998, Branch et al., 2000). These short-term (i.e., <1 wk) cultures have limited capacity to generate robust networks since *in vitro* cultures take weeks (>21 days) to fully develop mature axon connections (Dichter., 1978, Brewer et al., 1993). For these reasons, microfluidic structures such as microchannels (or tunnels) for the physical isolation of neuronal cells have been intensively investigated to generate long-term cultured neural networks (Claverol-Tinture and Pine., 2002, Bani-Yaghoub et al., 2005, Morin et al., 2005, Ravula et al., 2006, Dworak and Wheeler., 2009). While much progress has been made, the short distance of axons (≤500 μm) in these small neural circuits are not ideal for axon tract accessibility.

To establish functional connectivity of a neural circuit, two physically separated but axonally connected neuronal assemblies are expected to exhibit temporally related activities characteristic of their neuronal compositions. Those studies are routinely performed in live brain slices taking advantage of the well-established directionality of *in vivo* axon pathways. *In vitro* studies typically use multi-electrode arrays (MEAs) to record extracellular potential or current changes consequent of neuronal firing. These multi-electrode recordings detect network activity changes and signal transmission, including action potential propagation (Dworak and Wheeler., 2009), network synchronization (Takayama et al., 2012) and interaction (Kanagasabapathi et al., 2011). Though useful for providing network-level analysis, MEA signals from cultured circuits lack characteristic patterns, and difficult to relate to biochemical and molecular events in single cells, such as channel protein deficits in axon injury (Iwata et al., 2004,Yuen et al., 2009).

Recently, a long-length (2 mm) axon tract culture system (Tang-Schomer et al., 2010) was established as an *in vitro* model for studying diffuse axonal injury after brain trauma. This model allows for examination of dynamic changes of axons (Tang-Schomer et al., 2010) and dendrites (Monnerie et al., 2010), such as mechanical injury-induced undulations and beading, that are similar to the pathological presentations of patient brains (Tang-Schomer et al., 2012). An earlier version of compartmentalized cultures, in which axons grew as 2 mm-

wide networks, was used to identify sodium channel cleavage as a potential molecular mechanism for brain trauma-related functional deficits (Iwata et al., 2004, Yuen et al., 2009). Micropatterning techniques were introduced to this model (Tang et al.,, 2005) to examine axon-tract specific changes in morphology (Tang-Schomer et al., 2010) as well as channel protein deficits (Tang-Schomer et al, 2009). While promising, the existing model lacks the ability to detect electrophysiological changes.

In this study, we sought to integrate the unique design feature of long distance axon tracts of our model with the capabilities of electrophysiological and pharmacological manipulations into a multi-functional device. To design the fabrication process, we aim to incorporate conventional bioanalytical methods that are readily available in neuroscience laboratories, so that the device can be easily adapted for other models of axon tract-associated CNS disorders. Here, we demonstrate an array of four paired two-node connections of 2 mm-long axon tracts that are integrated on planar MEAs. Local perturbation of the circuit was demonstrated with microfluidic application of live cell dyes as well as targeted electrical stimulation to individual nodes of the network. Functional connectivity was evaluated by local application of neurotransmitters to one node and patch clamping of neurons in an axonnally connected node. These results present a robust network with integration capabilities with pharmacological and electrical manipulation at individually addressable unit of the circuit. The scalability of the microfabrication process and compatibility with standard *in vitro* bioassays of this system would make this system a useful tool for axon injury studies.

2. Materials and Methods

2.1. Microfabrication

Computer-aided designs (AutoCAD software, Autodesk Inc., San Rafael, CA, USA) were printed into transparency photomasks (Advance Reproduction Corp., Andover, MA, USA). Silicon wafers (100 mm dia., 500-550 um thick, <111>, Cemat Silicon SA, Warsaw, Poland) with micropatterned SU8 molds were generated with two-layer lithography procedures on a mask aligner (OAI Model 204IR, San Jose, CA, USA). Polydimethylsiloxane (PDMS, Sylgard 184, Dow Corning, MI, USA) was spin-coated onto silicon wafers with a spin coater (Model WS-400B-6NPP/LITE, Laurell Technologies Corp., North Wales, PA, USA). After curing for 1-4 hr at 60°C, thin PDMS masks were peeled off the wafer. The PDMS film-mask was also used for sputter coating gold MEAs (60-100 nm thickness) using a NSC-3000 sputter coater (Nano-Master Inc., Austin, TX, USA).

2.2. Silk film MEAs fabrication

2.2.1. Silk films—Silk films were processed as previously reported (Amsden et al., 2010, Gil et al., 2010). Briefly, a 100 μl solution of silk fibroin (1-2%) extracted from cocoons of the Bombyx mori silkworm (Tajima Shoji Co., Yokohama, Japan) were dried onto PDMS molds (14 mm dia., 0.5-1 mm thick). The silk film was peeled off the molds, contacted with a PDMS film-mask, and sputter-coated with gold MEAs. Silk film MEAs were subsequently water-annealed, UV sterilized, and coated with 20 μg/ml poly-L-lysine (Sigma-Aldrich, St. Louis, MO, USA) overnight, washed and dried prior to introducing cells.

2.2.2. Silk film MEAs—A new method was developed to incorporate gold wires into the silk film MEAs. Thin gold wires (25 μm dia., SPM Inc., Armonk, NY, USA) were threaded through a PDMS film mask and immersed in silk solution. With the PDMS film mask in place, the dried silk film was sputter coated with gold MEAs. After separation from the

PDMS mask, the silk film bore embedded gold wires that were connected with the patterned MEAs on its surface.

2.3. Primary cortical neuronal culture

The brain tissue isolation protocol (#Moss lab) was approved by Tufts University Institutional Animal Care and Use Committee and complies with the NIH Guide for the Care and Use of Laboratory Animals. Cortical neurons were prepared from embryonic day 18 rat (Sprague-Dawley rat, Charles River, Wilmington, MA, USA) embryos of either sex as previously described (Kittler et al., 2004; Jacob et al., 2005). Dissociated cells were plated at a density of 375,000 to 500,000 cells/cm2 and cultured in NeuroBasal media (Invitrogen, Carlsbad, CA, USA) supplemented with B-27 neural supplement (Invitrogen) and 5% fetal bovine serum (HyClone, Logan, UT, USA). Cultures were maintained in 37°C, 100% humidity and 5% CO2 in an incubator (Forma Scientific, Marietta, OH, USA) for up to 28 days *in vitro* (DIV30). Prior to cell plating, micropatterned PDMS film masks were placed onto a substrate of glass coverslips, polystyrene culture plates or silk film MEAs that were pre-coated with poly-L-lysine (0.1 mg/ml, overnight).

2.4. Immunocytochemistry

Fixed cells (4% paraformaldehyde) were permeabilized (0.1% Triton X-100) and incubated in a primary antibody solution (1:500-1000 dilution) overnight at 4 °C, followed with a secondary antibody (1:200-500 dilution) incubation for 1 hr at room temperature, and extensively washed. Immunostained cultures were viewed under a fluorescence microscope (Leica DM IL; Leica Microsystems, Wetzlar, Germany) equipped with a digital camera (Leica DFC340 FX). Primary antibodies of mouse monoclonal anti-glial fibrillary acidic protein (GFAP) (1:1000; Sigma) and rabbit polyclonal anti-βIII-tubulin (b3TB) (1:500; Sigma) were used. Goat anti-mouse and anti-rabbit Alexa 488 or 568 (1:250; Invitrogen) secondary antibodies were then applied. Fluorescence images were acquired using excitation/emission (Ex/Em) of 470/525 nm for Alexa 488, and Ex/Em of 560/645 nm for Alexa 568.

2.5. Live dye application to patterned primary cortical neuron cultures

Live cell tracers, Calcein-AM and Calcein Orange-AM, and lipophilic dyes, DiI and DiO (Invitrogen) were used. One μl dye solutions (cell tracers, 1 μg/ml in PBS with 1% DMSO; lipophilic dyes, 20 μg/ml in PBS with 1% DMSO) were applied to each mini-well of patterned cultures sequentially. After a 10 minute incubation at 37°C, the cultures were washed with phosphate-buffered saline (PBS) and incubated in fresh culture media for another 10 minutes, and viewed under a fluorescence microscope. Fluorescence images were acquired at Ex/Em of 470/525 nm for Calcein-AM and DiO, and 560/645 for Calcein Orange and DiI.

2.6. GFP transfection of primary cortical neurons

GFP plasmid was delivered into neuronal cultures at DIV2 using magnetic nanoparticles and oscillating magnetic fields (magnetofection) (McBain et al., 2008) (Magnefect-nanoTM, nanoTherics Ltd., Staffordshire, United Kingdom). The mammalian expression plasmid carrying a GFP reporter gene under the control of a cytomegalovirus (CMV) immediate early promoter/enhancer (pLenti CMV GFP Blast, 8322 bp, Addgene #17445, Cambridge, MA, USA) was complexed with neuMAG particles (dia. 100 nm, nanoTherics Ltd.). The plasmids were mixed with neuMAG particles at a ratio of 0.64 μg: 1.2 μl per well of a 24-well plate. The cultures were subjected to magnetofection at 2 Hz and 0.2 mm displacement for 30 min, and subsequently replaced with fresh medium. GFP expression was examined at

72 hr up to 10 days post-transfection, and fluorescence images were acquired at Ex/Em of 470/525 nm.

2.7. Electrical stimulation

To connect the integrated live neural circuit to external devices, a custom-made array of four gold pins (1 mm dia., 2 mm pitch, Digi-Key Corp., Thief River Falls, MN, USA) were placed in direct contact with the peripheral contact pads of the MEAs. The PDMS mask remained in place to insulate the cell-free regions of the MEAs. A functional generator (Tenma Universal Test Center 72-5085, MCM Electronics, Centerville OH, USA) delivered stimulus signals consisting of biphasic square waves of 160mV (peak-to-peak) and 20, 200 or 2k Hz for a duration of 2 min. Oscilloscope testing confirmed no signal loss at the electrodes inside the mini-wells. The voltage potential (160 mV) was applied between the gold pads with a reference electrode that was immersed in the solution. No heat generation or cellular damage was observed within the time-window of the stimulation experiment.

2.8. Calcium imaging and image analysis

Calcium dye Fluo-4 AM (Invitrogen) was used to visualize changes in intracellular calcium concentration. Cultures were loaded with 1 μg/ml dye solution (in PBS containing 0.2% DMSO) at 37°C for 30 min, washed with PBS, and incubated in fresh media for another 30° min. Fluorescence images were acquired before and immediately after stimulation under the same optical settings (at Ex/Em of 470/525 nm) and imaging conditions. Fluorescence change over a same region of interest was quantified using

$$\Delta F/F = [(Fi - Bi) - (F0 - B0)/(F0 - B0)$$

Where F0 and Fi are emission intensity before and after stimulation respectively, and Bi and B0 are fluorescence background following analogous notation.

2.9. Patch clamp

For electrophysiological measurements, neurons on coverslips were placed in a recording chamber mounted on the stage of an inverted microscope and continuously perfused with extracellular solution containing the following (in mM): 150 NaCl, 4.7 KCl, 2.5 $CaCl_2$, 1.2 $MgCl_2$, 10 HEPES, and 11 glucose, adjusted to pH 7.4 with NaOH, with osmolality 295–315 mmol/kg. Whole-cell recordings were carried out at 32 °C using recording chamber and in-line perfusion heaters (Warner Instruments, Hamden, CT). Patch pipettes were pulled from borosilicate glass (World Precision Instruments) and filled with intracellular solution containing the following (in mM): 140 KCl, 2 $MgCl_2$, 0.1 $CaCl_2$, 10 HEPES, 1.1 EGTA, 2.5 creatine phosphate and 2 Mg-ATP, adjusted to pH 7.4 with KOH, with osmolality 275–290 mmol/kg. After establishing whole-cell conditions, an incubation period of 3 to 5 min was allowed to stabilize recordings before collecting data. Recordings were made at a holding potential of −60 mV. Action potential (AP) currents were continuously recorded using an Axopatch 200B amplifier (Molecular Devices), low-pass filtered at 2 kHz, digitized (10 kHz; Digidata 1320A; Molecular Devices), and stored for off-line analysis. Access resistance (<15 MΩ; 65–75% compensation) was monitored throughout the recordings, and data from the cell were discarded when a change of >20% occurred. Frequencies of AP currents were analyzed from selected 30 s epochs, using Mini Analysis software (Synaptosoft). Unless indicated otherwise, data are expressed as mean ± SEM; p values represent the results of t tests.

Coverslips containing cortical neurons were placed in the recording chamber such that the flow of extracellular solution in the chamber was perpendicular to the axis of the axonal tracts. Cortical neurons plated in the lower microwell were used to record AP currents using the whole-cell configuration of the patch-clamp technique. γ-Aminobutyric acid (GABA, 10 uM) was applied to cortical neurons from the upper microwell via a fast-step, three barrel perfusion system (SF-77B Warner Inst.). The perfusion system produces a horizontal step with the time between adjacent barrels being approximately 20 ms with each barrel having an inner diameter of 0.7 mm. The opening to the first barrel is positioned above the patterned cortical neurons from the upper microwell. Extracellular solution flowed through the first two barrels and GABA flowed through the third barrel (Fig. 5A). Two to five minutes of continuous recording was made with extracellular solution focally applied to the cortical neurons from the upper microwell before manually switching over to GABA application for a further five minutes.

3. Results

3.1. Integrated multi-electrode arrays (MEAs) with living neuronal circuits

3.1.1. Integrated MEAs on hard surfaces—The integrated circuit was composed of a microfabricated PDMS mask and compartmentalized neuronal culture on a planar substrate (Figure 1). PDMS mask fabrication started with (1) computer aided design (CAD) of a parallel array of pads connected by a ladder of millimetre-long micropatterns. After two-layer lithography (2), a silicon wafer was generated with SU8 photoresist features consisting of a first layer (50-100 μm height) corresponding to the micropatterns and a second layer of a greater height (200-500 μm) corresponding to the pads. Fig. 1a shows an example of 50 μm wide and 2 mm long micropatterns conjoining two arrays of circular posts of 50 μm dia. and 300 μm heights. Liquid PDMS was spin-coated (3) under a controlled speed to cover the wafer such that the liquid immerses the first layer of SU8 features but levels at or below the second layer. Fig. 1b shows a representative region of cured PDMS embedding an array of circular posts of 50 μm dia. and 300 μm heights. Thermal-cured PDMS was peeled off the wafer as a film-like mask with through-holes and micropatterns on its surface, and formed a conformal contact with a planar substrate (4). The holes in the PDMS mask formed mini-wells to expose the underneath surfaces for cell plating, while the micropatterns formed microchannels to permit axon outgrowth (5). Fig. 1c shows a representative fluorescence image of a compartmentalized neuronal culture. Two separated neural cell populations, co-immunostained with neuronal marker, β3 tubulin (β3TB, green) and glial cell marker, glial fibrillary acidic protein (GFAP, red), were connected with an array of 2 mm-long β3TB+ axon tracts growing in 50 μm wide channels. On a substrate with MEAs (6), the electrodes placed underneath the holes are extended to peripheral contact electrodes, which provided a direct access to connect with electronic stimulation and/or recording systems.

3.1.2. Integrated MEAs on silk films—In addition to a hard surface such as glass coverslips and polystyrene culture plates, this technology also applies to flexible and ultra-thin (2-5 μm) silk films (Amsden et al., 2010,Gil et al., 2010). MEA arrays were sputter-coated onto dried silk films; and gold wires can be embedded in the silk films during film-processing to connect MEA components to external devices (see Methods). This formed flexible, transparent, self-supporting film-based MEAs. Fig. 1d shows an example that was suspended on a water drop.

3.2. Dimension designs of neuronal cell and axon tract compartments

3.2.1. Designs of neuronal cell compartments—We used CAD to design dimensions of cell compartments and microchannels for optimal neuronal culture (Figure 2). Examination of cell densities in the cell compartment, i.e., the mini-wells, showed an

increasing tendency of cell aggregation as the density increased. Fig. 2A shows representative fluorescence images of Calcein AM-stained neuronal cultures at 16 days *in vitro* (DIV 16) in a 1.5 by 1.5 mm mini-well. Cells plated at ∼130 k/cm2 formed dispersed monolayers (a), at ∼530 k/cm2 forming small clusters (b), and at 1 mil/cm2 large clusters formed and axon bundles aligned along the boundaries of the mini-well (c). The last scenario was found to be difficult for axons to extend into the microchannels. For the smallest sized mini-well tested, 50 μm dia. circular wells, only cell clumps were found settled inside after the initial plating and were also unable to extend long axons into the microchannels (data not shown).

3.2.2. Designs of axon tract compartments—To determine the effect of channel dimensions on axon track formation, the width of the channels was altered to 400, 200, 100 and 50 μm, and the length to 2 mm and 3 mm. Fig. 2B shows representative fluorescence images of β3TB immunostained axons at DIV 21 in microchannels of different widths. Axons extended a 2 mm length between DIV 7-10, and a 3 mm length between DIV 21-28. Once the connections were established, the tracts remained stable for more than 4 weeks. In 400 μm-wide channels, individual processes intermingled with thick axon fascicles, and showed a zigzagging path with a preference towards the two edges of the channel walls (Fig. 2d). As the channel width decreased from 200 μm to 100 μm, there was less zigzagging and a lower degree of fasciculation at the channel walls (Fig. 2e and f). As the channel width decreased to 50 μm and as the length increased to 3 mm, axons showed a strong tendency to fasciculate (Fig. 2g, h): Axons entered into the channels as individually identifiable processes and converged into a thick bundle in the greater middle portion of the channel.

3.2.3. GFP transfection of axon tracts—GFP plasmid transfection of the neural cell circuit allowed for visualization of complex axon trajectories by staining only a small fraction of cells so that individual neurons could be identified (Fig. 2C). Figure 2C, i is a representative fluorescence image of a 1 mm by 0.8 mm region (∼ the surface area of an entire mini-well), showing three GFP+ neurons (“1”, “2”, “3”) and their intertwined axonal network. A neuron may extend its axon into a distant microchannel bypassing nearby channels, as shown in Fig. 2j. The inset shows an overlay of GFP+ axon segment onto a phase contrast image of the dense neuronal culture in the background. Individual neurons extended axons in multiple directions as seen in Fig. 2k in which multiple GFP+ processes originating from one neuron travel independently in a 100 μm channel.

3.3. Local drug application to targeted neuronal populations at different nodes of a circuit

As a proof-of-concept of local drug applications to targeted neuronal populations in a circuit without exposure to more distant neural populations, we applied live cell dyes into separated mini-wells on the same substrate (Figure 3). Fig. 3A is a representative fluorescence image of a circuit showing patterned neuronal populations independently absorbing two different cell permanent calcein-AM dyes. Once cleaved by intracellular esterase, the dyes were retained in the cytoplasm, allowing observation of dye absorption in the cell compartment. In this example, three pairs of mini-wells (“a-b”,”c-d”, “e-f”) received ∼1μL red, green, green, red, green and red calcein-AM dye solutions, respectively. Little mixing of the dyes occurred during the 10 min incubation and subsequent ∼10 min PBS washes and media replacement steps, despite the presence of microchannels that connected each pair. In an alternative application, we used lipophilic dyes, DiI (red) and DiO (green). Once incorporated into the cell membrane, these dyes were rapidly transported inside and along axons, allowing for observation of dye absorption in the axon compartments. Fig. 3B shows representative fluorescence images of two connected neuronal populations absorbing DiI and DiO at different time points, respectively. In this example, the left-side population was applied with the red dye (DiI) first, and the right-side population with the green dye (DiO) at

a later time point. As the delay increased from the top lane going downward, mixed absorption of dyes was observed in the axon tracts with an increasing red-to-green gradient. At the interface zone where DiI and DiD solutions met (Fig. 3k, l; arrows indicating microfluidic flow direction of DiI, red and DiD, green), two distinctive populations of neurons showed different uptake of DiI versus DiD.

3.4. Local electrical stimulation to targeted neuronal populations at different nodes of a circuit

For electrical stimulation of the living neuronal circuit, biphasic square waves of 160 mV (peak-to-peak) and 20, 200 or 2000 Hz were applied for a 5-min duration, and intracellular calcium changes were examined before and immediately after stimulation, using a fluorescence calcium indicator, fluo-4 (Figure 4). To deliver electrical stimulation, a custom-made array of four gold pins to connect the peripheral contact electrodes of the MEA to a functional generator (Fig. 4A, see Methods) was used. Fig. 4A shows a representative fluorescence photograph of fluo-4 stained cortical neurons growing on and near gold (Au) surface electrode (outlined in yellow). Fig. 4B depicts representative 'heat-map' images converted from fluorescence photographs of fluo-4 stained cortical neurons before and after electrical stimulation, showing increased intensity under 20 Hz (a and b) and diminished intensity under 2000 Hz (c and d). The intensity changes occurred to neurons near the Au electrode in a highly localized distribution. Fig. 4C shows quantification of fluo-4 intensity changes of neurons under different stimulation frequencies. Under 20 Hz stimulation, neurons showed ∼46% increases in fluorescence intensities ($n = 14$, $p = 0.008$ compared to before stimulation, **, $p<0.01$, Student's t-test). In contrast, there was a ∼22% decrease under 2k Hz stimulation ($n = 16$, $p = 0.008$ compared to before stimulation; **, $p<0.01$, Student's t-test). There were no significant change under 200 Hz stimulation ($n = 6$, $p = 0.53$ compared to before stimulation).

3.5. Functional connectivity of patterned neuronal populations in the circuit

We next wanted to examine if axon tracts from one population of patterned cortical neurons had functional connections with another population of patterned cortical neurons (Figure 5). We used the whole-cell configuration of the patch-clamp technique to record action potential (AP) currents from the lower patterned cortical neurons while stimulating the upper patterned cortical neurons approximately 2 mm apart but joined by axonal tracts (Fig. 5A). Application of 10 μM γ-aminobutyric acid (GABA) resulted in a significant increase in AP firing frequency from 0.6 ± 0.12 Hz to 1.4 ± 0.29 Hz ($n = 5$; $p = 0.03$, Fig. 5B & C) without affecting the AP amplitude. When axon tracts were cut, no change in AP frequency was observed with the application of GABA (data not shown). These data demonstrate that changing the circuit behavior in one population of patterned cortical neurons, with the application of GABA, altered the circuit behavior of a separate population of patterned cortical neurons via functional axonal connectivity.

4. Discussion

A living neural circuit integrated with MEAs was developed that is suitable for functional studies of axon tract systems. The living neural circuit consists of individually addressable neuronal cell populations and arrays long distance axon tracts on planar electrode arrays that can be interfaced with external electrical devices. Design parameters were characterized to select the physical dimensions of the cell compartments for promoting a mono-layer cell culture, and the microchannels for stable long-term growth of axon tracts. In addition, fabrication of the circuit can be adapted to flexible substrate such as ultra-thin silk fibroin-based films. The millimeter scale separation of cell compartments allows local perturbations of targeted neuronal populations, including microfluidic drug applications and MEA-

transmitted electrical stimulation. The results showed controlled selectivity of dye absorption by different neurons. MEA-transmitted electrical stimulation of targeted neurons showed ~46% increase of intracellular calcium levels with 20 Hz stimulation, but ~22% decrease with 2k Hz stimulation. Local application of the neurotransmitter γ-aminobutyric acid (GABA) to one node induced increased action potential firing rate of neurons in a physically separated but axonally connected node, suggesting the axon tracts to be inhibitory afferents. This easy-to-adapt platform has the capability of being integrated with a variety of analytical methods across molecular, cellular and system levels, and would provide opportunities for functional studies of axon tracts in a neural circuit *in vitro*.

4.1. Millimeter-scale node-to-node separation

To adapt state-of-the-art measures of basic cellular processes or molecular events that are key mediators of neural network function, one desirable property of a circuit is to have the structural features compatible with standard bio-analytical methods, such as immunostaining, live cell imaging and electrophysiological examinations. In particular, for network-level modulations, it is critical to be able to perturb one node and evaluate a distant node simultaneously. Microfluidic structures coupled on planar MEAs can provide microscale precision for multisite electrical manipulation of a defined neural circuit. However, the short distance (≤500 μm) of axons in current existing systems require microfluidic setup to achieve fluid isolation between compartments during pharmacological manipulation (Takayama et al., 2012, Kanagasabapathi et al., 2011). By comparison, the millimeter scale node-to-node distance in our system allows for separated microfluidic absorption by multiple compartments. Though the channel size in this study is significantly large for microfluidic control within a channel (<5 μm) (Takayama et al., 1999), a two millimeter separation combined with a time scale of cellular uptake in seconds limited mixed cellular absorption of dyes, as shown in Figure 3. In addition, individual neurons and axons can be identified and monitored in the optimized mono-layer culture. This feature is useful to relate single cell-based analysis to network-level behavior.

4.2. Long-length axon tract formation

In this living neural circuit, ordered axon tracts connecting separated neuronal populations as well as paired surface electrodes were formed to mimic reciprocal projections in the CNS (Hevner et al., 2002). Close-walled microchannels provide a permanent spatial confinement for long-term (>2 wks), high density, and long length growth of axons, as compared to open surface patterns for short-term (<1 wk), low density and short distance axon alignment (Kleinfeld et al., 1988, Ravenscroft., 1998, Jun et al., 2007, Branch et al., 2000). Such high density axon growth in a confined space showed a tendency toward *in vivo*-like fasciculation. Surprisingly, the axons did not always extend to the closest but rather wound into a distant microchannel, as shown with GFP-expressing single neurons. This phenomenon indicates that physical confinement, though necessary for blocking alternative paths, may not be sufficient for dictating an axon projection. Considering that axons within a cortical bundle are functionally related (Sperry., 1963, Imai et al., 2009), this finding suggests the axon tracts in an *in vitro* circuit may be of different functional specialization depending on their intrinsic properties. This behavior could be harnessed to determine the functional connectivity in-between different nodes of the circuit, i.e., a functional map, in relation to their geometrical arrangement, i.e., a physical map.

4.3. Functional connectivity: inhibitory afferents

Studies of axon tract formation in mammalian brain have found complex intermingling and regional preferences of axon trajectories depending on their relative positions in the originating and target areas, as well as specific points within tracts (Lehman et al., 2011).

With a mixed culture of dissociated whole-brain cortical neurons, an alternative approach would be to use electrophysiological features to determine the functional identity of a specific axon tract. In this study, patch clamp recordings show that application of inhibitory neurotransmitter GABA in one population of cortical neurons increased action potential firing frequencies of a distant neuronal population via functional axonal connections. Normally, increasing GABA at the neuronal synapse inhibits the generation of the action potential of the neuron, thereby making it less likely to excite nearby neurons. Though the observation of increased neuronal activity may seem conflicting with the inhibitory role of GABA, it is possible to explain the mechanism via activation of inhibitory afferents. Specifically, GABA suppressed inhibitory neurons at the node where it was applied, and sent depressed output via the projection axons to neurons in the connecting node. Decreased input from these inhibitory afferents would lead to increased excitability of the connected neurons. The time-related stimulus-responses of two separated nodes provide evidence for their functional connectivity associated with their axonal connections. These findings also suggest that a long-term cortical culture may comprise of a large percentage of inhibitory neurons, as implicated by their delayed enrichment in *in vitro* cultures (Hayashi et al., 2003).

4.4. Electrical stimulation

The machine-interface capability of the living neural circuit is demonstrated by electrical stimulation-induced calcium changes of the targeted neurons. Electrical stimulation is of particular interest given its clinical use as an effective treatment for Parkinson's disease (Olanow et al., 2000) and depression (Mayberg et al., 2005) and is currently explored as a therapeutic measure for PTSD after traumatic brain injury (Novakovic et al., 2011). In this study, intracellular calcium levels, indicated by fluo4 fluorescence intensity, showed a ∼46% increase under 20 Hz biphasic stimulation, ∼22% decrease under 2k Hz, and a highly localized effect in neurons only in the vicinity of the electrode. Since calcium influx occurs immediately upon neuronal activation (Berridge., 1998, Balkowiec and Katz., 2002), these findings suggest that low frequency stimulation activated the targeted cortical neurons and high frequency stimulation inhibited them. This result is consistent with deep brain stimulation studies for Parkinson's, for which it was found that stimulation at 200- and 350-Hz diminished β- oscillations and reduced the severity of parkinsonian symptoms (Kuhn et al., 2008), whereas low frequency (∼13-30 Hz) activated the stimulated region (MacKinnon et al., 2005, McConnell et al., 2012). To examine how electrical stimulation induced calcium signaling at the cellular level relates to oscillation changes of neural network activities, recording from the MEA electrodes will be necessary in conjunction with single cell-based patch clamping. While sufficient for electrical stimulation, the current MEA design in this system is not ideal for recording due to low impedance from the large surface area of each electrode. Nevertheless, compared to other neural circuit systems that rely on pre-configured commercial MEA chips, the scalable and adaptable microfabrication process in our system can readily configure MEA designs to match for different compartmentalization and interface needs.

4.5. Conclusion: Application for axon injury studies

This easy-to-adapt platform has integrated capabilities of pharmacological and electrophysiological manipulations. The large number of axons in this system could be extracted to provide protein and RNA-level analysis for identifying molecular targets, similarly as with the previous version of this model (Iwata et al., 2004, Yuen et al., 2009). In the context of diffuse axonal injury, the capability of fabrication on flexible substrates could support force induction to mimic the mechanical conditions experienced by the axons during traumatic brain injury (Smith et al., 1999, Tang-Schomer et al., 2010). Together, the newly modified model could allow for assessments of multiple endpoints including axon tract tracing, calcium influx, action potential, network architecture and activities. These

properties make this system a useful tool as a multi-functional platform for studying axon tract-associated CNS disorders *in vitro*.

Acknowledgments

We thank Dr. Robert White and Tufts Microfabrication Laboratory for providing cleanroom assistance, and Dr. Omenetto Fiorenzo, Dr. Marie Tupai, and Joe Marturano for discussions. We thank Dr. Steve Moss's laboratory at Tufts Center of Neuroscience for providing embryonic rat brain tissues and the electrophysiological equipment. Preliminary work pertaining to the development of compartmentalized neuronal culture was carried out by M.D.T. in Dr. Douglas Smith's laboratory at the University of Pennsylvania, using a lithographic design developed by M.D.T. in Dr. Joe Tien's laboratory at Boston University. This work was funded by NIH (P41 Tissue Engineering Resource Center EB002520, EY020856) and Tufts Center for Neuroscience Research Core Award to M.D.T.

References

Adams JH, Doyle D, Ford I, Gennarelli TA, Graham DI, McLellan DR. Diffuse axonal injury in head injury: definition, diagnosis and grading. Histopathology. 1989; 15:49–59. [PubMed: 2767623]

Amsden JJ, Domachuk P, Gopinath A, White RD, Negro LD, Kaplan DL, Omenetto FG. Rapid nanoimprinting of silk fibroin films for biophotonic applications. Adv Mater. 2010; 22:1746–9. [PubMed: 20496408]

Balkowiec A, Katz DM. Cellular mechanisms regulating activity-dependent release of native brain-derived neurotrophic factor from hippocampal neurons. J Neurosci. 2002; 22:10399–407. [PubMed: 12451139]

Bani-Yaghoub M, Tremblay R, Voicu R, Mealing G, Monette R, Py C, Faid K, Sikorska M. Neurogenesis and neuronal communication on micropatterned neurochips. Biotechnol Bioeng. 2005; 92:336–45. [PubMed: 16094670]

Berridge MJ. Neuronal calcium signaling. Neuron. 1998; 21:13–26. [PubMed: 9697848]

Branch DW, Wheeler BC, Brewer GJ, Leckband DE. Long-term maintenance of patterns of hippocampal pyramidal cells on substrates of polyethylene glycol and microstamped polylysine. IEEE Trans Biomed Eng. 2000; 47:290–300. [PubMed: 10743770]

Brewer GJ, Torricelli JR, Evege EK, Price PJ. Optimized Survival of Hippocampal Neurons in B27-Supplemented Neurobasalm, a New Serum-free Medium Combination. J Neurosci Methods. 1993; 35:567–76.

Christman CW, Grady MS, Walker SA, Holloway KL, Povlishock JT. Ultrastructural studies of diffuse axonal injury in humans. J Neurotrauma. 1994; 11:173–86. [PubMed: 7523685]

Claverol-Tinture E, Pine J. Extracellular potentials in low-density dissociated neuronal cultures. J Neurosci Methods. 2002; 117:13–21. [PubMed: 12084560]

Corey JM, Feldman EL. Substrate patterning: an emerging technology for the study of neuronal behavior. Exp Neurol. 2003; 184(1):S89–96. [PubMed: 14597331]

Corey JM, Wheeler BC, Brewer GJ. Compliance of hippocampal neurons to patterned substrate networks. J Neurosci Res. 1991; 30:300–7. [PubMed: 1798054]

Dichter MA. Rat cortical neurons in cell culture: culture methods, cell morphology, electrophysiology, and synapse formation. Brain Res. 1978; 149:279–93. [PubMed: 27283]

Dworak BJ, Wheeler BC. Novel MEA platform with PDMS microtunnels enables the detection of action potential propagation from isolated axons in culture. Lab Chip. 2009; 9:404–10. [PubMed: 19156289]

Friesen WO. Reciprocal inhibition: a mechanism underlying oscillatory animal movements. Neurosci Biobehav Rev. 1994; 18:547–53. [PubMed: 7708368]

Gentleman SM, Roberts GW, Gennarelli TA, Maxwell WL, Adams JH, Kerr S, Graham DI. Axonal injury: a universal consequence of fatal closed head injury? Acta Neuropathol. 1995; 89:537–43. [PubMed: 7676809]

Ghosh A, Sydekum E, Haiss F, Peduzzi S, Zorner B, Schneider R, Baltes C, Rudin M, Weber B, Schwab ME. Functional and anatomical reorganization of the sensory-motor cortex after incomplete spinal cord injury in adult rats. J Neurosci. 2009; 29:12210–9. [PubMed: 19793979]

Gil ES, Park SH, Marchant J, Omenetto F, Kaplan DL. Response of human corneal fibroblasts on silk film surface patterns. Macromol Biosci. 2010; 10:664–73. [PubMed: 20301120]

Hammarback JA, Palm SL, Furcht LT, Letourneau PC. Guidance of neurite outgrowth by pathways of substratum-adsorbed laminin. J Neurosci Res. 1985; 13:213–20. [PubMed: 3973933]

Hayashi K, Kawai-Hirai R, Harada A, Takata K. Inhibitory neurons from fetal rat cerebral cortex exert delayed axon formation and active migration in vitro. J Cell Sci. 2003; 116:4419–28. [PubMed: 13130100]

Hevner RF, Miyashita-Lin E, Rubenstein JL. Cortical and thalamic axon pathfinding defects in Tbr1, Gbx2, and Pax6 mutant mice: evidence that cortical and thalamic axons interact and guide each other. J Comp Neurol. 2002; 447:8–17. [PubMed: 11967891]

Imai T, Yamazaki T, Kobayakawa R, Kobayakawa K, Abe T, Suzuki M, Sakano H. Pre-target axon sorting establishes the neural map topography. Science. 2009; 325:585–90. [PubMed: 19589963]

Iwata A, Stys PK, Wolf JA, Chen XH, Taylor AG, Meaney DF, Smith DH. Traumatic axonal injury induces proteolytic cleavage of the voltage-gated sodium channels modulated by tetrodotoxin and protease inhibitors. J Neurosci. 2004; 24:4605–13. [PubMed: 15140932]

Jun SB, Hynd MR, Dowell-Mesfin N, Smith KL, Turner JN, Shain W, Kim SJ. Low-density neuronal networks cultured using patterned poly-l-lysine on microelectrode arrays. J Neurosci Methods. 2007; 160:317–26. [PubMed: 17049614]

Jung DR, Kapur R, Adams T, Giuliano KA, Mrksich M, Craighead HG, Taylor DL. Topographical and physicochemical modification of material surface to enable patterning of living cells. Crit Rev Biotechnol. 2001; 21:111–54. [PubMed: 11451046]

Kanagasabapathi TT, Ciliberti D, Martinoia S, Wadman WJ, Decre MM. Dual-compartment neurofluidic system for electrophysiological measurements in physically segregated and functionally connected neuronal cell culture. Front Neuroeng. 2011; 4:13. [PubMed: 22025913]

Kleinfeld D, Kahler KH, Hockberger PE. Controlled outgrowth of dissociated neurons on patterned substrates. J Neurosci. 1988; 8:4098–120. [PubMed: 3054009]

Kuhn AA, Kempf F, Brucke C, Gaynor Doyle L, Martinez-Torres I, Pogosyan A, Trottenberg T, Kupsch A, Schneider GH, Hariz MI, Vandenberghe W, Nuttin B, Brown P. High-frequency stimulation of the subthalamic nucleus suppresses oscillatory beta activity in patients with Parkinson's disease in parallel with improvement in motor performance. J Neurosci. 2008; 28:6165–73. [PubMed: 18550758]

Lehman JF, Greenberg BD, McIntyre CC, Rasmussen SA, Haber SN. Rules ventral prefrontal cortical axons use to reach their targets: implications for diffusion tensor imaging tractography and deep brain stimulation for psychiatric illness. J Neurosci. 2011; 31:10392–402. [PubMed: 21753016]

Li N, Tourovskaia A, Folch A. Biology on a chip: microfabrication for studying the behavior of cultured cells. Crit Rev Biomed Eng. 2003; 31:423–88. [PubMed: 15139302]

MacKinnon CD, Webb RM, Silberstein P, Tisch S, Asselman P, Limousin P, Rothwell JC. Stimulation through electrodes implanted near the subthalamic nucleus activates projections to motor areas of cerebral cortex in patients with Parkinson's disease. Eur J Neurosci. 2005; 21:1394–402. [PubMed: 15813949]

McConnell GC, So RQ, Hilliard JD, Lopomo P, Grill WM. Effective deep brain stimulation suppresses low-frequency network oscillations in the Basal Ganglia by regularizing neural firing patterns. J Neurosci. 2012; 32:15657–68. [PubMed: 23136407]

Monnerie H, Tang-Schomer MD, Iwata A, Smith DH, Kim HA, Le Roux PD. Dendritic alterations after dynamic axonal stretch injury in vitro. Exp Neurol. 2010; 224:415–23. [PubMed: 20478308]

Morin FO, Takamura Y, Tamiya E. Investigating neuronal activity with planar microelectrode arrays: achievements and new perspectives. J Biosci Bioeng. 2005; 100:131–43. [PubMed: 16198254]

Novakovic V, Sher L, Lapidus KA, Mindes JA, Golier J, Yehuda R. Brain stimulation in posttraumatic stress disorder. Eur J Psychotraumatol. 2011; 2 Epub 2011 Oct 17. 10.3402/ejpt.v2i0.5609

Olanow CW, Brin MF, Obeso JA. The role of deep brain stimulation as a surgical treatment for Parkinson's disease. Neurology. 2000; 55:S60–6. [PubMed: 11188977]

Rauch SL, Shin LM, Phelps EA. Neurocircuitry models of posttraumatic stress disorder and extinction: human neuroimaging research--past, present, and future. Biol Psychiatry. 2006; 60:376–82. [PubMed: 16919525]

Ravenscroft MSS. Developmental neurobiology implications from fabrication and analysis of hippocampal neuronal networks on patterned silane-modified surfaces. J Am Chem Soc. 1998; 120:12169–77.

Ravula SK, McClain MA, Wang MS, Glass JD, Frazier AB. A multielectrode microcompartment culture platform for studying signal transduction in the nervous system. Lab Chip. 2006; 6:1530–6. [PubMed: 17203157]

Smith DH, Wolf JA, Lusardi TA, Lee VM, Meaney DF. High tolerance and delayed elastic response of cultured axons to dynamic stretch injury. J Neurosci. 1999; 19:4263–9. [PubMed: 10341230]

Sperry RW. Chemoaffinity in the Orderly Growth of Nerve Fiber Patterns and Connections. Proc Natl Acad Sci U S A. 1963; 50:703–10. [PubMed: 14077501]

Strich SJ. Diffuse degeneration of the cerebral white matter in severe dementia following head injury. J Neurol Neurosurg Psychiatry. 1956; 19:163–85. [PubMed: 13357957]

Takatsuru Y, Fukumoto D, Yoshitomo M, Nemoto T, Tsukada H, Nabekura J. Neuronal circuit remodeling in the contralateral cortical hemisphere during functional recovery from cerebral infarction. J Neurosci. 2009; 29:10081–6. [PubMed: 19675241]

Takayama S, McDonald JC, Ostuni E, Liang MN, Kenis PJ, Ismagilov RF, Whitesides GM. Patterning cells and their environments using multiple laminar fluid flows in capillary networks. Proc Natl Acad Sci U S A. 1999; 96:5545–8. [PubMed: 10318920]

Takayama Y, Moriguchi H, Kotani K, Suzuki T, Mabuchi K, Jimbo Y. Network-wide integration of stem cell-derived neurons and mouse cortical neurons using microfabricated co-culture devices. BioSystems. 2012; 107:1–8. [PubMed: 21872639]

Tang-Schomer MD, Patel AR, Baas PW, Smith DH. Mechanical breaking of microtubules in axons during dynamic stretch injury underlies delayed elasticity, microtubule disassembly, and axon degeneration. FASEB J. 2010; 24:1401–10. [PubMed: 20019243]

Tang-Schomer MD, Johnson VE, Baas PW, Stewart W, Smith DH. Partial interruption of axonal transport due to microtubule breakage accounts for the formation of periodic varicosities after traumatic axonal injury. Exp Neurol. 2012; 233:364–72. [PubMed: 22079153]

Tang-Schomer MD, Reyn K, Patel AR, Meaney D, Smith DH. Modulation of proteolytic susceptibility of sodium channels through microtubule stabilization in traumatic axonal injury. (Abstract) National Neurotrauma Society Meeting. 2009 Sep.

Tang, MD. PhD thesis. Boston University; 2005. A tissue-engineered microvascular network.

Taylor AM, Blurton-Jones M, Rhee SW, Cribbs DH, Cotman CW, Jeon NL. A microfluidic culture platform for CNS axonal injury, regeneration and transport. Nat Methods. 2005; 2:599–605. [PubMed: 16094385]

Yuen TJ, Browne KD, Iwata A, Smith DH. Sodium channelopathy induced by mild axonal trauma worsens outcome after a repeat injury. J Neurosci Res. 2009; 87:3620–5. [PubMed: 19565655]

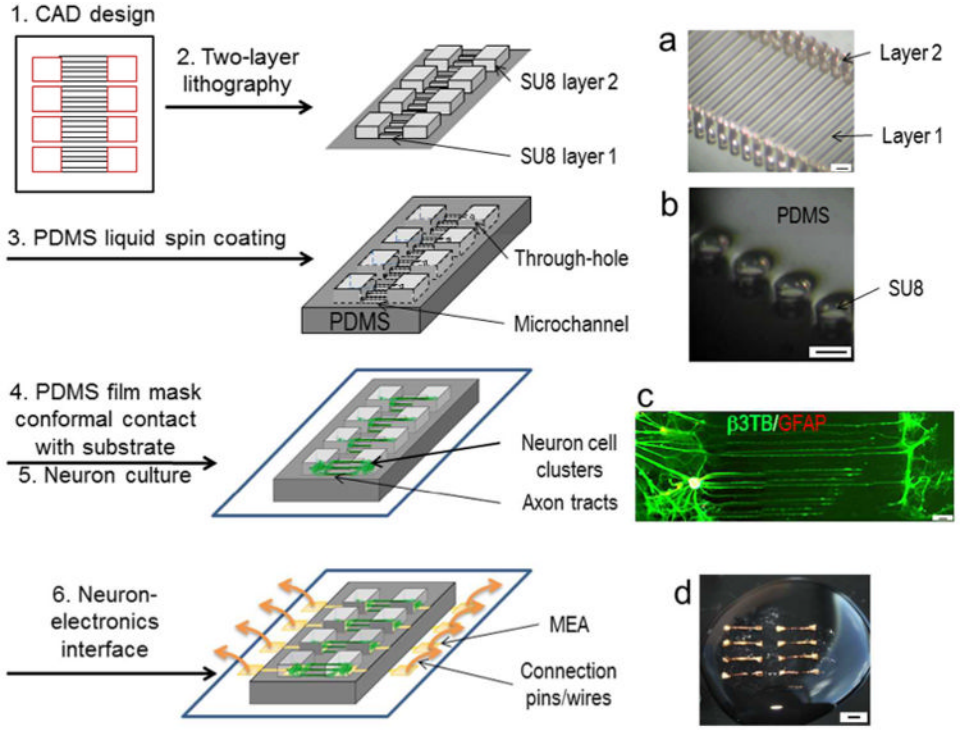

Figure 1. Fabrication of a living neuronal circuits, schematics and representative photographs

(1) Computer aided design (CAD) of a parallel array of pads connected by a ladder of millimeter-long micropatterns. **1a**. Light microscopic photograph of a silicon wafer with SU8 features of 50 μm wide and 2 mm long micropatterns (Layer 1) conjoining two arrays of circular posts of 50 μm dia. and 300 μm height (Layer 2). **(2)** Two-layer lithography. A silicon wafer with SU8 photoresist features consisting of a first layer of micropatterns and a second taller layer of pads. **(3)** Spin-coating of liquid PDMS to cover the first layer of SU8 features but not the second layer. **1b.** Light microscopic photograph of spin-coated and thermal-cured PDMS embedding an array of circular posts of 50 μm dia. and 300 μm height. **(4)** Thermal-cured PDMS as a film mask to make a conformal contact with a planar substrate, and **(5)** for compartmentalized neuronal culture: Cells are confined in the mini-wells and axons form tracts in the microchannels. **1c.** A representative fluorescence photograph of a compartmentalized neuronal culture, co-immunostained with neuronal marker, β3 tubulin (β3TB, *green*) and glial cell marker, glial fibrillary acidic protein (GFAP, *red*). Scale bars: 50 μm. **(6)** Interface of the living neuronal circuit with a substrate with MEAs. **1d.** A circuit on a thin silk protein-based film. Scale bars: 2 mm.

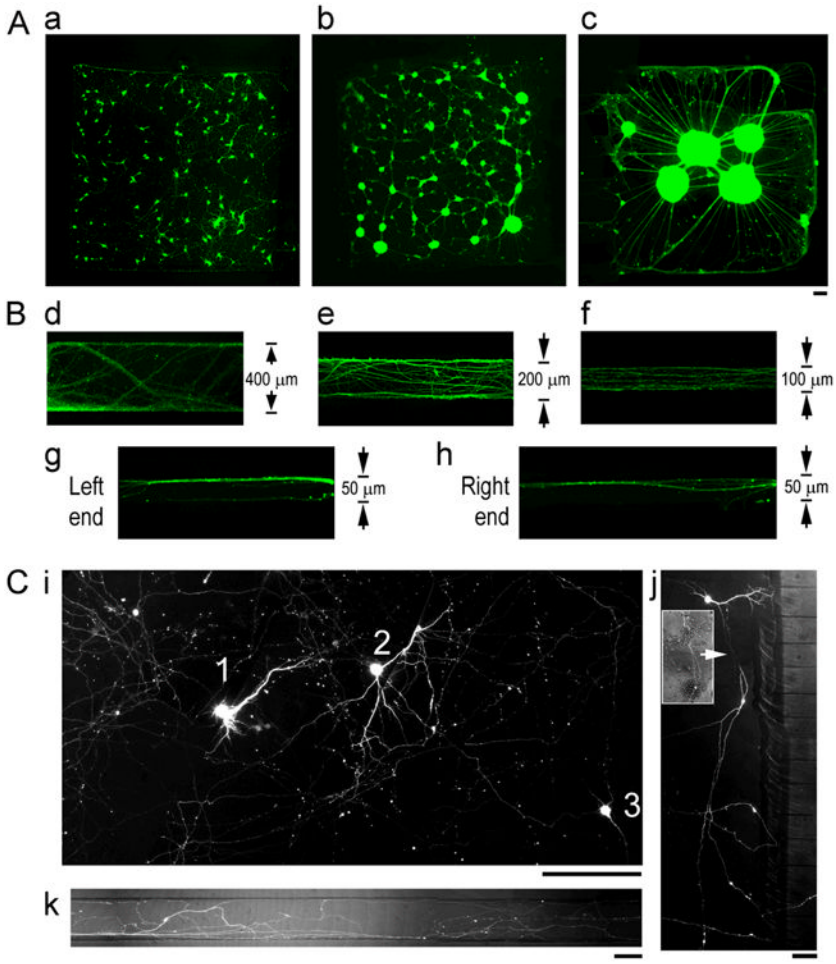

Figure 2. Dimension designs of neuronal cell and axon compartments

(A) Fluorescence photographs of Calcein-AM stained (*green*) neuronal cultures at DIV 16 in a 1.5 by 1.5 mm mini-well of different plating densities, 130 k/cm^2(**a**), 530 k/cm^2(**b**), 1 mil/cm^2(**c**). Scale bar: 100 μm **(B)** Fluorescence photographs of β3TB-immunostained axons at DIV 16-21 in microchannels of different widths, 400 μm **(d)**, 200 μm **(e)**, 100 μm **(f)**, and 50 μm **(g)** of the Left end (**g**), and the Right end (**h**) of a channel. **(C)** Representative fluorescence photograph of GFP+ neurons and axons in a circuit, showing complex axon trajectory. (**i**) Three GFP+ neurons (**“1”, “2”, “3”**) in an entire region of a mini-well. **(j)** A GFP+ neuronextending its axon (arrow) into a distant microchannel bypassing nearby channels. Inset shows overlay of GFP+ axon segment onto phase contrast image of a dense neuronal culture in the background. **(l)** Multiple GFP+ axon processes derived from a same neuron in a 100 μm channel. Scale bars: 100 μm.

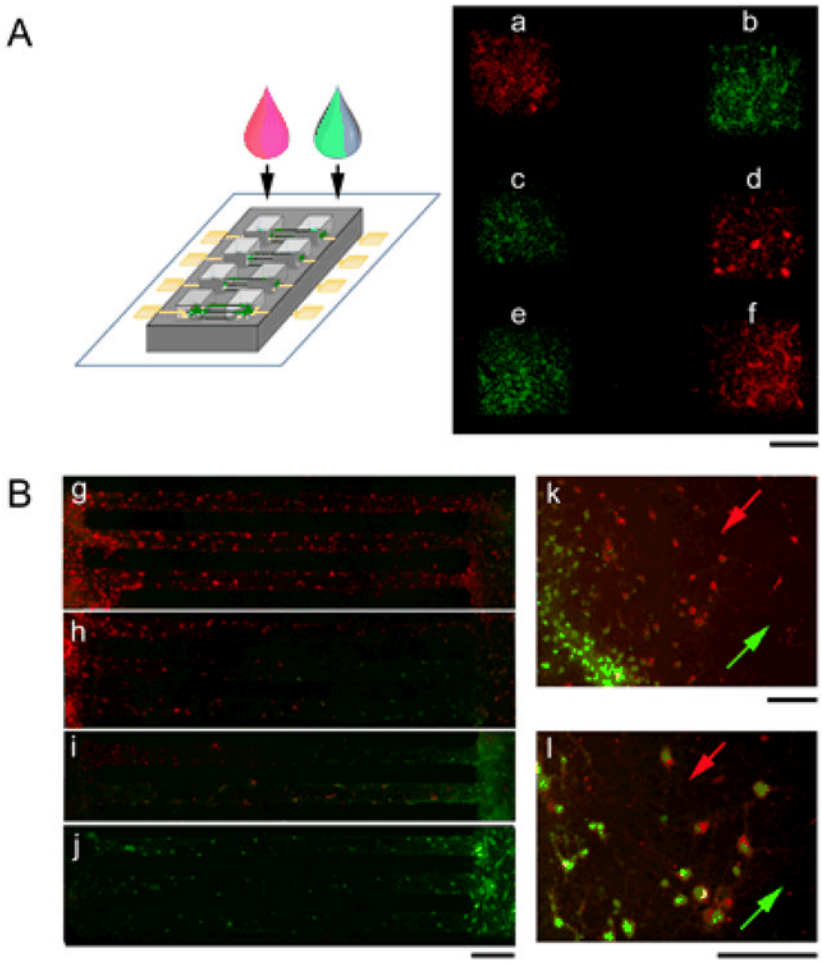

Figure 3. Local drug application to targeted neuronal populations at different nodes of a circuit

(A) Left: Schematics of applying dye solutions to different mini-wells of a circuit. **Right**: A representative fluorescence photograph of a substrate with six mini-wells ("**a**", "**b**", "**c**", "**d**", **"e", "f"**) after application of calcein-AM dye solutions of different fluorescence spectrum (red and green), showing little mixing in the microchannels that connected **a** to **b**, **c** to **d**, and **e** to **f.** Scale bars: 500 μm **(B)** Fluorescence photographs of two connected neuronal populations absorbing DiI (*red*) and DiD (*green*) at different time points, the left-side population applied with DiI first and the right-side population with DiO at a later time point with increased delay from the top lane going downward (**g, h, i, j**). The interface zone where DiI and DiD solutions met (**k, l**; arrows indicating microfluidic flow direction of DiI, *red* and DiD, *green*), show two distinctive populations of neurons that absorbed DiI vs. DiD. Scale bars: 100 μm.

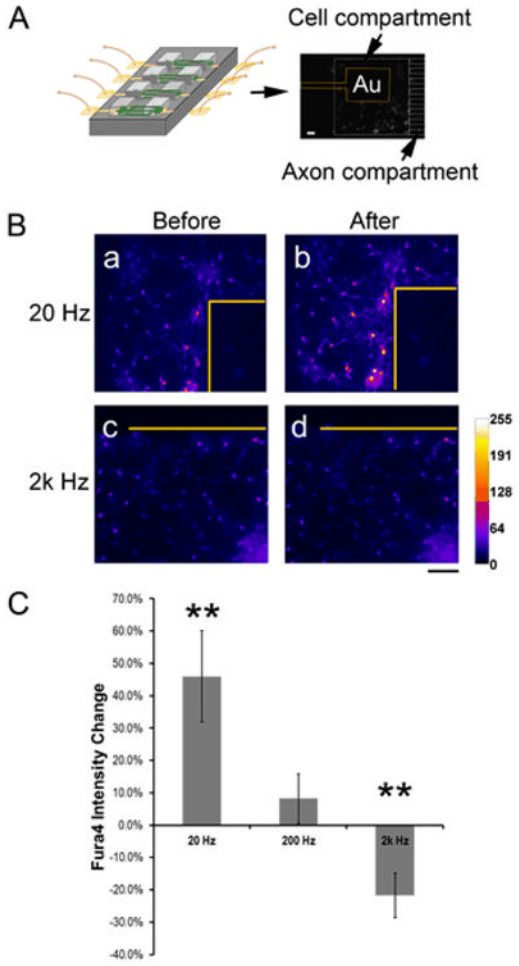

Figure 4. Local electrical stimulation to targeted neuronal populations at different nodes of a circuit

(A) Left: Schematics of interfacing MEAs of the circuit to a custom-made array of gold pins that connects to a functional generator. **Right**: A representative fluorescence photograph of fluo-4 stained cortical neurons growing on and near a gold (Au) surface electrode (outlined in yellow). The mini-well and microchannels are outlined in white dashed lines. Scale bar: 150 μm. Scale bar: 150 μm. **(B)** Representative 'heat-map' images converted from fluorescence photographs of fluo-4 stained cortical neurons before and after electrical stimulation, showing increased intensity under 20 Hz (**a** and **b**) and diminished intensity under 2000 Hz (**c** and **d**). Note the highly localized intensity changes near the Au electrodes (outline in yellow). Scale bar: 100 μm. **(C)** Quantification of frequency-dependent fluorescence changes of fluo-4 stained neurons (20 Hz, n = 14, $p = 0.008$; 2k Hz, n = 6, $p = 0.53$; **, $p<0.01$, Student's t-test, compared to before stimulation).

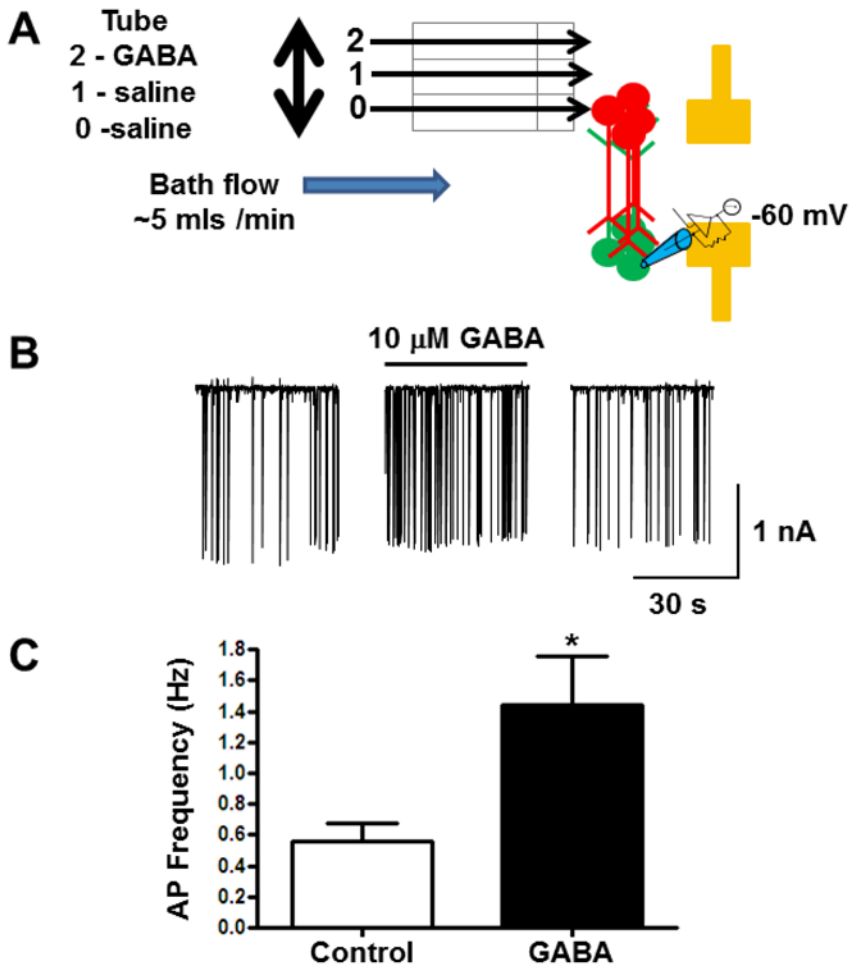

Figure 5. Functional connectivity of patterned neuronal populations in the circuit

(A) Diagram of experimental set up. Flow of extracellular solution in the recording chamber (∼5 mls/min) was perpendicular to the axis of the axonal tracts Extracellular solution flowed through the first two tubes and GABA flowed through the third barrel. The opening to the first barrel is positioned above the patterned cortical neurons from the upper microwell. AP currents were recorded from cortical neurons in the lower microwell. (**B)** Example of action potential currents recorded from cortical neurons. Application of 10 μM GABA resulted in a significant increase in AP firing frequency. (**C)** Average frequency of AP currents recorded from neurons before and after application of 10 μM GABA (n = 5/group; *, $p = 0.03$).